Michaud, D. P., Gupta, S. C., Whalen, D. L., Sayer, J. M., & Jerina, D. M. (1983) *Chem.-Biol. Interact. 44*, 41–52.
Moore, P. D., Koreeda, M., Wislocki, P. G., Levin, W., Conney, A. H. Yagi, H., & Jerina, D. M. (1977) *ACS Symp. Ser. 44*, 127–154.
Osborne, M. R., Jacobs, S., Harvey, R. G., & Brookes, P. (1981) *Carcinoenesis (London) 2*, 553–558.
Pulkrabek, P., Leffler, S., Weinstein, I. B., & Grunberger, D. (1977) *Biochemistry 16*, 3127–3132.
Pulkrabek, P., Leffler, S., Grunberger, D., & Weinstein, I. B. (1979) *Biochemistry 18*, 5128–5134.
Slaga, T. J., Bracken, W. M., Viaje, A., Levin, W., Yagi, H., Jerina, D. M., & Conney, A. H. (1977) *Cancer Res. 37*, 4130–4133.
Slaga, T. J., Bracken, W. M., Gleason, G., Levin, W., Yagi, H., Jerina, D. M., & Conney, A. H. (1979) *Cancer Res. 39*, 67–71.
Undeman, O., Lycksell, P. O., Graslund, A., Astlind, T., Ehrenberg, A., Jernstrom, B., Tjerneld, F., & Norden, B. (1983) *Cancer Res. 43*, 1851–1860.
Wang, A. H. J., Quigley, G. J., Kolpak, F. J., Crawford, J. L., van Boom, J. H., van der Marel, G., & Rich, A. (1979) *Nature (London) 282*, 680–686.
Weinstein, I. B., Jeffrey, A. M., Jennette, K. W., Blobstein, S. H., Harvey, R. G., Harris, C., Autrup, H., Kasai, H., & Nakanishi, K. (1976) *Science (Washington, D.C.) 193*, 592–595.
Yagi, H., Thakker, D. R., Hernandez, O., Koreeda, M., & Jerina, D. M. (1977) *J. Am. Chem. Soc. 99*, 1604–1611.
Yang, N. C., Hrinyo, T. P., Petrich, J. W., & Yang, D. H. (1983) *Biochem. Biophys. Res. Commun. 114*, 8–13.
Zimmerman, S. B., Cohen, G. H., & Davies, D. R. (1975) *J. Mol. Biol. 92*, 181–192.

Secondary Structure of a 345-Base RNA Fragment Covering the S8/S15 Protein Binding Domain of *Escherichia coli* 16S Ribosomal RNA†

Joanne M. Kean and David E. Draper*
Department of Chemistry, Johns Hopkins University, Baltimore, Maryland 21218
Received October 2, 1984

ABSTRACT: A technique for isolating defined fragments of a large RNA has been developed and applied to a ribosomal RNA. A section of the *Escherichia coli rrn*B cistron corresponding to the S8/S15 protein binding domain of 16S ribosomal RNA was cloned into a single-stranded DNA phage; after hybridization of the phage DNA with 16S RNA and digestion with T_1 ribonuclease, the protected RNA was separated from the DNA under denaturing conditions to yield a 345-base RNA fragment with unique ends (bases 525–869 in the 16S sequence). The secondary structure of this fragment was determined by mapping the cleavage sites of enzymes specific for single-stranded or double-helical RNA. The fragment structure is almost identical with that proposed for the corresponding region of intact 16S RNA on the basis of phylogenetic comparisons [Woese, C. R., Gutell, R., Gupta, R., & Noller, H. (1983) *Microbiol. Rev. 47*, 621–669]. We conclude that this section of RNA constitutes an independently folding domain that may be studied in isolation from the rest of the 16S RNA. The structure mapping experiments have indicated several interesting features in the RNA structure. (i) The largest bulge loop in the molecule (20 bases) contains specific tertiary structure. (ii) A region of long-range secondary structure, pairing bases about 200 residues apart in the sequence, can hydrogen bond in two different mutually exclusive schemes. Both appear to exist simultaneously in the RNA fragment under our conditions. (iii) The long-range secondary structure and one adjacent helix melt between 37 and 60 °C in the absence of Mg^{2+}, while the rest of the structure is quite stable.

Much of our understanding of RNA secondary and tertiary structure comes from extensive physical studies of tRNA. Most other cellular RNAs are at least an order of magnitude larger and have been much less amenable to structural studies. However, in the last few years an abundance of sequence information has made it feasible to search for RNA secondary structures by comparing sequences of the same RNA specie from different organisms: as the sequence varies, pairs of compensating base changes are observed, which preserve the base pairing of some potential helices (Noller, 1980; Noller & Woese, 1981). This "phylogenetic" approach has been extensively applied to ribosomal RNAs, and there is now substantial agreement on the secondary structures of these molecules (Woese et al., 1983; Maly & Brimacombe, 1983).

The availability of plausible secondary structures has been a major advance in the study of large RNA molecules; however, detailed studies of tertiary structures, conformational transitions, and protein–RNA interactions in RNAs of >1000 bases are still intimidating to contemplate. We have considered the possibility that large RNA molecules are organized into independently folding domains which may be studied individually. For the best studied of the larger RNAs, the *Escherichia coli* 16S ribosomal RNA, it has been suggested that the RNA is organized into three major structural domains that each bind specific sets of the ribosomal proteins and fold (to a first approximation) independently (Zimmermann, 1974). Many fragments of ribosomal RNAs do retain their ability

† This research was supported by National Institutes of Health Grant GM-29048 and by Grant BRSG S07 RR7041 awarded by the Biomedical Research Support Program, Division of Research Resources, National Institutes of Health.

0006-2960/85/0424-5052$01.50/0

to interact specifically with purified proteins (Zimmermann et al., 1972; Ungewickell et al., 1975; Tritton & Crothers, 1976). Thus, it may be possible to study a large RNA piecewise if specific structural domains can be isolated.

In this paper we report a method, based on recombinant DNA techniques, for preparing specific, well-defined fragments of a large RNA in good yield. Our first application has been with the region of *E. coli* 16S RNA known to interact directly with ribosomal proteins S8 and S15. This potential structural domain is about 200 bases in length, and phylogenetic comparisons predict nine helices in the secondary structure (Woese et al., 1983). We find from structure mapping experiments that these helices exist in a 345-base fragment covering this region. The experiments also suggest that some regions of the fragment have specific tertiary structures.

Materials and Methods

Chemicals and Enzymes. Water was distilled and run through a "Milli-Q" deionizer and filter. Baker reagent grade formamide was filtered through Whatman No. 42 paper, run over Dowex 50 1-X8 mixed-bed deionizing resin until the conductivity was above 10000 Ω/cm, and finally filtered through 0.2-μm polycarbonate filters (Nuclepore Corp.). Other chemicals were standard reagent grade. ^{32}P nucleotides were purchased from Amersham. Enzymes and polyacrylamide gel reagents were obtained from BRL, except proteinase K and calf intestinal phosphatase (Boehringer-Mannheim) and cobra venom V_1 nuclease (P-L Biochemicals).

Buffers and Media. TE buffer is 10 mM tris(hydroxymethyl)aminomethane (Tris)[1] and 1 mM EDTA, pH 7.6. TBE buffer contains 0.1 M Tris, 0.1 M boric acid, and 2 mM Na_2EDTA, pH 8.3. All solutions were either autoclaved or filtered through 0.45-μm sterile membranes (Gelman). Glassware was baked at 180 °C, and plasticware at 95 °C, overnight. M9–glycerol growth medium is M9 minimal medium (Maniatis et al., 1982) with 0.4% glycerol replacing the glucose.

Preparation and Growth of fd Phase Clones. All procedures for restriction digests of DNA, isolation of DNA fragments, ligations, transformations, and selection of antibiotic resistant bacteria were standard (Maniatis et al., 1982). The *E. coli* strain HB101 (Boyer & Roulland-Dussoix, 1969) was used throughout. A DNA fragment from the *E. coli rrn*B cistron, corresponding to nucleotides 528–867 in the 16S RNA sequence, was obtained from a *Fnu*DII (CG|CG) digest of the plasmid pKK3535 (Brosius et al., 1981). This fragment was ligated into *Sma*I (CCC|GGG) cut fd106 phage replicative form. (fd106 contains an insertion of kanamycin and ampicillin resistance genes; Herrmann et al., 1980.) Fourteen kanamycin sensitive transformants were isolated, and the phage was DNA tested for hybridization to [^3H]16S rRNA (Dennis & Nordan, 1976). All 14 showed strong hybridization. Replicative form DNA was isolated from two of the isolates, and the identity and orientation of the inserted DNA were confirmed by restriction analysis. This phage is F61. We have no good explanation for why this fragment of DNA was found in only one orientation; other DNA restriction fragments from overlapping regions of the 16S rDNA insert equally well in either orientation in the same vector.

We were unable to prepare F61 phage DNA by infection of male bacteria as the insert appears to delete rapidly. We prepared the DNA by first transforming *E. coli* HB101 with the F61 replicative form and then picking individual colonies from agar plates into M9–glycerol medium. The bacteria were grown for 24 h at 37 °C with vigorous aeration in shaker flasks. After the bacteria were pelleted, the phage were purified by precipitating with polyethylene glycol and banding in CsCl density gradients (Yamamoto et al., 1970). DNA was isolated from the phage by two phenol extractions in TE buffer and ethanol precipitation. The usual yield was about 2 mg of single-stranded DNA/L of culture; up to 5 mg/L is obtained with other phage clones by this protocol.

Preparation of F61 Hybrid. In a typical preparation 1 nmol of F61 DNA was hybridized with 1.5 nmol of 16S RNA in 1 mL of TE buffer plus 0.4 M NaCl for 20 min at 65 °C. Then 6000 units of ribonuclease T_1 was added and incubation continued for 2 h at 37 °C. Adding proteinase K to 100 μg/mL and SDS to 0.5% inactivated the ribonuclease after 1.5 h at 37 °C. This mixture was run over a 1.5 × 45 cm Sephacryl S-500 (Pharmacia) gel filtration column equilibrated with TE buffer plus 0.2 M NaCl. The peak DNA fractions were pooled and ethanol precipitated.

^{32}P End Labeling of the RNA and Isolation of the Fragment. The DNA–RNA hybrids could be 5′ end labeled with [^{32}P]ATP and polynucleotide kinase or 3′ labeled with cytidine [^{32}P]bisphosphate and RNA ligase by using standard reaction conditions (D'Alessio, 1981). Prior to 3′ labeling the hybrid was dephosphorylated with calf intestinal phosphatase in the buffer recommended by the supplier at 56 °C for 15 min followed by phenol extraction. A total of 20 pmol of hybrid was incubated at 37 °C for 40 min in 30 μL total volume for 5′ end labeling, or at 4 °C overnight in 30 μL for 3′ labeling. After either end-labeling reaction the hybrid was precipitated with 15 μL of 7.5 M ammonium acetate and 135 μL of ethanol. The pelleted DNA was resuspended in 40 μL of TE buffer and diluted with 10 μL of 1 M Tris, pH 7.6, 20 μL of 10% SDS, and 0.45 mL of formamide. After being warmed to 65 °C for 5 min, the melted hybrid was applied to a 4-cm slot in a 2 mm thick × 20 cm long 5% polyacrylamide/50% urea gel made up and run in 40 mM Tris, 40 mM sodium acetate, and 1 mM EDTA, pH 8.0. The gel was run at 150 V for about 3 h and autoradiographed and the band of labeled RNA cut out. To extract RNA from the excised portion of gel, we obtained optimum results by first freezing the gel between layers of parafilm at −70 °C, squeezing the gel, and then extracting it with 0.5 M ammonium acetate and 0.1 mM EDTA at 37 °C overnight (D'Alessio, 1981). The RNA was phenol extracted and ethanol precipitated twice with 50 μg of poly(A) as carrier; it was finally stored in 0.2 M NaCl and 10 mM Tris, pH 7.6.

We were able to separate the RNA from DNA by applying the melted hybrid to a 1 × 25 cm Sephacryl S-500 column equilibrated with 80% formamide, 10 mM HEPES pH 7.6, and 1 mM EDTA. The peak of RNA fragment was concentrated by precipitation with 50 μg of poly(A) as carrier, 0.3 M sodium acetate, and 3.5 volumes of ethanol at −20 °C. This RNA was phenol extracted and ethanol precipitated as with the gel-purified material.

Sequencing Gels and Reactions. Sequencing gels were 85 cm long and 0.4 mm thick, prepared from 8% acrylamide and 50% urea in TBE buffer as described by Maxam & Gilbert (1980). Gels were run at 30–40 W constant power for as long as 16 h. Preflashed Kodak X-Omat R X-ray film was exposed to the gel at −70 °C (Laskey, 1982). In most cases a Du Pont Cronex intensifying screen was used, but better resolution of closely spaced bands was obtained without the screen. When required, a Joyce-Loebl Chromoscan 3 densitometer was used

[1] Abbreviations: RNase, ribonuclease; Tris, tris(hydroxymethyl)-aminomethane; EDTA, ethylenediaminetetraacetic acid; SDS, sodium dodecyl sulfate.

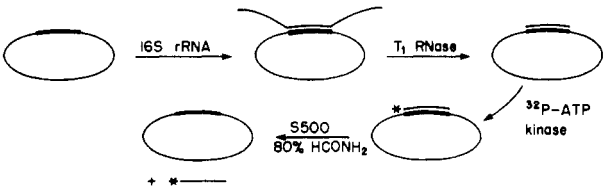

FIGURE 1: Scheme for the isolation of a defined fragment from a large RNA. See text for explanation.

to determine relative band intensities by using a 0.25 × 5 mm beam.

RNA was annealed for 5 min at 65 °C in storage buffer (0.2 M NaCl and 10 mM Tris, pH 7.6) before use in structure mapping experiments. A T_1 RNase digest in 6 M urea and an alkaline hydrolysis were run on every gel for reference (D'Alessio, 1981).

Results and Discussion

Isolation of RNA Fragment. The scheme we used to fragment 16S ribosomal RNA at specific points is shown in Figure 1. DNA corresponding to the desired region of RNA is cloned into a single-stranded DNA phage, and the resulting complementary DNA is used to prepare a hybrid with 16S RNA. Ribonuclease digestion in this hybrid is limited to the unwanted single-stranded tails of the RNA. The hybrid is end labeled with ^{32}P and denatured and the RNA fragment purified.

We have used two methods to separate the RNA fragment from the phage DNA after denaturation: gel filtration on a Sephacryl S-500 column in 80% formamide or electrophoresis on a 50% urea–5% acrylamide gel in a low-salt buffer (see Materials and Methods). The gel filtration method (Figure 2) is well suited for larger preparations (up to a nanomole of fragment), but it does not sharply separate RNA molecules of different size. Even 1% contamination with RNA fragments less than full length is a serious problem for structure mapping experiments. More homogeneous material is obtained from electrophoresis of the melted hybrid and excision of the full-length fragment from the gel.

We found that the strand separation temperature for the hybrid is 35–40 °C in our denaturation buffer. The gel filtration column and the electrophoresis are run at close to ambient temperatures (25 °C). However, renaturation is extremely slow in the low-salt buffer and has been a problem only when we have tried to electrophorese rather concentrated samples (>0.5 mg/mL phage DNA). Quantitation of the material in the RNA peak by hybridization to F61 DNA gives overall yields of >80%.

The F61 RNA is extremely fragile when labeled with ^{32}P, particularly at a few CpA bonds (e.g., at 620). For structure mapping experiments we have had to work fairly quickly with the RNA once it is labeled.

Primary Structure of the F61 RNA Fragment. The F61 phage clone (described under Materials and Methods) contains DNA complementary to bases 528–867 in the 16S RNA sequence (Noller & Woese, 1981). We have examined the termini of the corresponding F61 RNA fragment by running 15% acrylamide sequencing gels of 5′- and 3′-end-labeled material (data not shown). The RNA fragment covers bases 525–869, in accord with the G cutting specificity of the RNase T_1 used to generate the fragment.

E. coli has seven *rrn* cistrons coding for ribosomal RNAs; *rrn*B (Brosius et al., 1981) and part of *rrn*G (Shen et al., 1982) have been sequenced. There are some sequence differences between these, though not in the region we have isolated. Since we are preparing the F61 RNA fragment from total *E. coli*

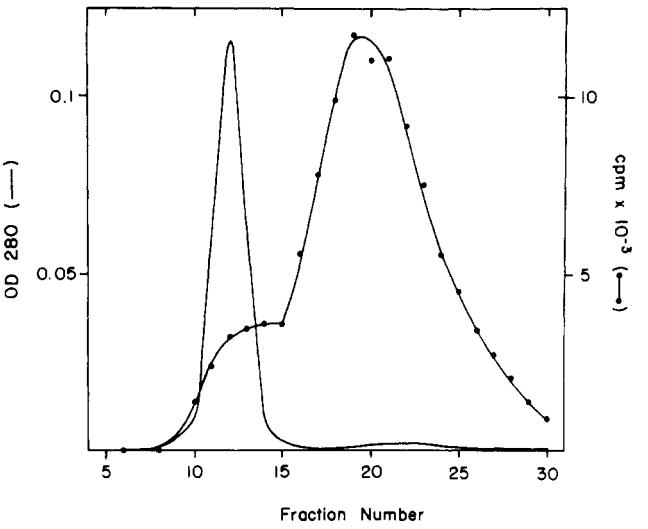

FIGURE 2: Gel filtration of F61 DNA–RNA hybrid under denaturing conditions. Sephacryl S-500 gel filtration in 80% formamide buffer was performed as described under Materials and Methods. Optical density was recorded in an Isco UV5 monitor by using a 5-mm flow cell. Aliquots of 20 μL were removed from collected fractions (0.7 mL) for scintillation counting.

16S RNA, there is the possibility that we are dealing with fragments of slightly different sequence. Our sequencing results (data not shown) using T_1 RNase (G specific), U_2 RNase (A specific), and *B. cereus* RNase (pyrimidine specific) agree with the *rrn*B sequence and do not detect any variants.

In two regions of our sequencing gels, bands are very closely spaced and difficult to unambiguously resolve. At 624–628 (with 5′ label) the band compression is clearly a consequence of a very stable G-C-rich hairpin (Figure 5). Bases 720–723 are compressed with 3′-end-labeled RNA, and there is the possibility of a hairpin between a C_5 sequence (735–739) and bases 721–725 (GGUGG, Figure 6).

Structure Mapping Experiments. The main goal of these experiments has been to map the secondary structure of the F61 RNA fragment for comparison with the structures proposed for intact 16S RNA. We have used three enzymes with different specificities to detect secondary structure. T_1 RNase is specific for single-stranded G residues; T_2 RNase is single stranded specific with little base specificity; cobra venom V_1 nuclease cuts only double-helical RNA (Auron et al., 1982; Lockard & Kumar, 1981). All digestions were done at pH 7.6. V_1 nuclease digestions have been done at 37 °C and several salt concentrations, ranging from 0.25 mM Mg^{2+} and 0.1 M Na^+ to 10 mM Mg^{2+} and 0.2 M Na^+ (Mg^{2+} cannot be entirely eliminated from V_1 nuclease digests). No significant difference between the digestion patterns was observed in this salt range. Because we wished to observe partial unfolding of the RNA fragment, T_1 and T_2 RNase digestions were standardly done in 0.1 M Na^+ with no Mg^{2+} present. T_1 RNase was used at both 37 and 60 °C and T_2 at 37 °C only. To make a valid comparison between the V_1 and T_1 nuclease digestions, 10 mM Mg^{2+} was added to some T_1 RNase digests at both 37 and 60 °C. As expected, Mg^{2+} substantially increases the stability of the RNA structure so that no denaturation is detected by T_1 RNase at the higher temperature. At 37 °C the addition of Mg^{2+} has no major effect on the T_1 RNase digestion pattern. These results will be discussed further below; the point to be made here is that Mg^{2+} does not induce a rearrangement of the RNA secondary structure. We cannot, of course, rule out the possibility that Mg^{2+} affects aspects of the tertiary structure of the molecule to which T_1 RNase is insensitive.

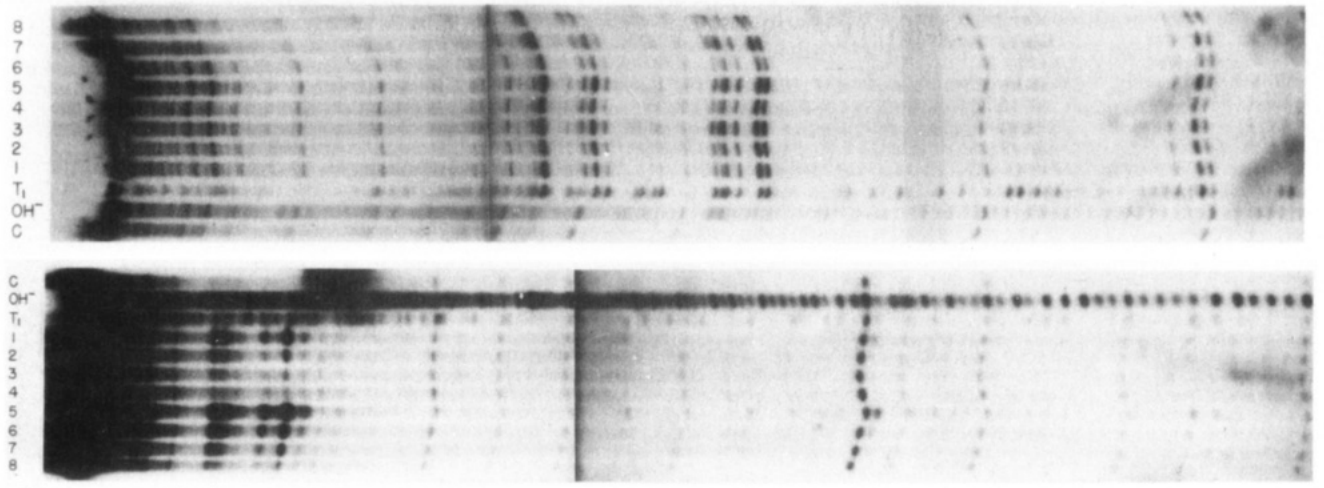

FIGURE 3: Denaturing polyacrylamide gels (85 cm) displaying the sensitivity of the F61 RNA fragment to T_1 RNase at 37 °C. Lanes present on both gels are the following: C, no enzyme added; OH^-, alkaline hydrolysis; T_1, T_1 RNase digestion under denaturing conditions. (Left) Gel using 3′-end-labeled material. Lanes 1–4 used 0.255 unit of T_1 RNase; lanes 5–8 used 0.128 unit. Lanes 1, 3, 5, and 7 were incubated for 1.5 min and the others for 3 min. Carrier RNA was 11.7 g of poly(A) in lanes 1, 2, 5, and 6 and 1.7 μg in the others. (Right) Gel using 5′-end-labeled material. Lanes 1, 2, 5, and 6 used 0.255 unit of T_1 RNase and the others 0.0128 unit. Incubation was for 5 min in lanes 1, 3, 5, and 7 and 1.5 min in the others. Carrier was 1.7 μg of poly(A) in lanes 1–4 and 11.7 μg in lanes 5–8.

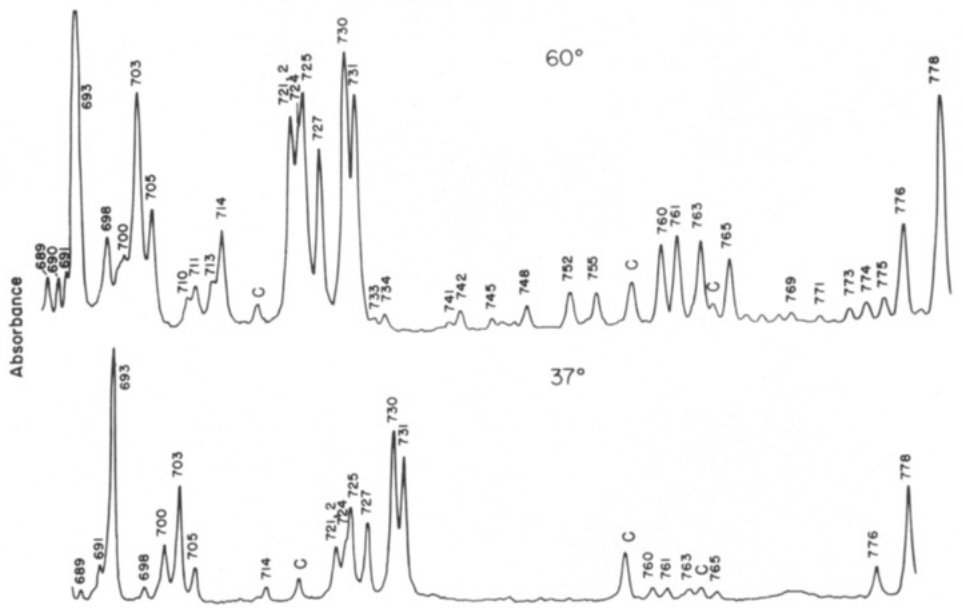

FIGURE 4: Densitometer scans of gel autoradiographs showing T_1 RNase reactivity of residues in the F61 RNA. Bases 688–778 are shown in each trace. G residues are numbered; C indicates that the peak is present in the control (undigested) lane as well. Upper trace, digestion at 60 °C; lower trace, digestion at 37 °C.

In the presentation of results that follows, a site is reported as sensitive to a nuclease only if it is found in independent experiments with different preparations of RNA. Garrett & Oleson (1982) have reported that cutting of 5S ribosomal RNA in certain locations causes a conformational change in the molecule that renders a normally inaccessible site extremely sensitive to certain nucleases; the phenomenon was detected by comparing the digestion patterns of 3′- and 5′-labeled RNA. We have therefore also attempted to trace each digestion pattern along the entire F61 sequence with both 5′- and 3′-end-labeled RNA. Although the precise location of cuts becomes ambiguous more than 200 bases from a terminus, the presence or absence of a band could generally be distinguished at up to 300 bases. We could not find any differences between 5′-end-labeled and 3′-end-labeled patterns. To ensure that any individual RNA molecule was not cut more than once, the amount of full-length material remaining after digestion was compared with an undigested control; only digestions that had >90% full-length molecules remaining were included in the analysis. Reactions were also done with different enzyme to RNA ratios and different digestion times to see whether relative cutting intensities changed markedly; no difference of this sort was observed as long as less than about 10% of the molecules had been cut (see Figure 3).

The data are summarized in Table I and Figures 5–8; note that cutting at a particular base position refers to hydrolysis of the phosphoester 3′ to that base. Because different bonds in the RNA vary considerably in susceptibility to an enzyme, gel autoradiographs were scanned in a densitometer, the highest peak assigned an intensity of 5 (T_1 and T_2 digests) or 4 (V_1 digests) and the intensity of the remaining peaks scaled accordingly. This is meant only to give a rough idea of the relative cutting rates at different sites. It has been particularly useful in objectively comparing T_1 RNase digests at 37 and 60 °C. Example densitometer scans are shown in Figure 4.

In the following sections we present a description of the data in Table I and compare our results with the predictions and results of other groups. For convenience we have divided the

Table I: Reactivity of Phosphodiester Bonds in the F61 RNA Fragment to Different Enzymes[a]

	enzyme					enzyme					enzyme					enzyme			
bond	T_1 (37 °C)	T_1 (60 °C)	T_2	V_1	bond	T_1 (37 °C)	T_1 (60 °C)	T_2	V_1	bond	T_1 (37 °C)	T_1 (60 °C)	T_2	V_1	bond	T_1 (37 °C)	T_1 (60 °C)	T_2	V_1
A560					C				*c*	A					C750				2
U					U				*c*	G	1	2			U				2
U					G				*c*	C					G		1		
A				1	G				*c*	G690		2			A				
C				2	G				*c*	G	1	2			C				
U				2	A				*c*	U			3		G		1		1
G	1	3		2	A630				*c*	G	5	5	2		C				
G	1	3		2	C					A			3		U				3
G	1	2			U					A			3		C				
C				2	G					A			2		A			1	1
G570		1		1	C					U					G760	1	2		1
U					A					G	1	2			G	1	2		1
A					U				1	C					U				
A					C				1	G700	1	2		2	G	1	2		
A					U				1	U			1		C				
G	1	3			G					A			2		G	1	2		3
C					A640					G	3	4			A			1	
G		2		1	U					A			1		A			1	
C				2	A					G	2	2			A				
A				2	C					A					G				
C580					U					U				1	C770				
G	1	3			G	1	2			C				2	G				2
C					G	1	2			U				1	U				
A				1	C				2	G710					G				1
G	1	3			A					G					G				1
G	1	3			A					A					G				2
C				1	G650		2			G		2			G	2	2		1
G	1	2		1	C					G	1	2			A			4	
G	1	3		1	U					A					G	3	4	1	
U					U					A					C				
U590				1	G	1	2			U					A780			1	
U				2	A					A				2	A			1	
G	1	3			G	1	1			C				*e*	A			1	
U					U				1	C720				*e*	C				1
U					C				3	G	1	2[d]		*e*	A				3
A					U				1	G				*e*	G		1		1
A					C660				1	U					G		1		
G					G					G	1	2	2	*f*	A			1	
U					U					G	2	4	2	*f*	U		2		
C					A					C			2		U			2	
A600					G	1	1			G	2	3		2	A790			5	
G				3	A				1	A			3		G	3	4	4	
A				3	G				2	A			4		A			4	
U				4	G				1	G730	4	4	3		U			2	
G				4	G				1	G	4	4			A			2	
U				1	G				2	C					C				
G		1[b]			G670				1	G					C				
A				2	G				1	G					C				1
A					U					C					U				3
U610					A					C				1	G				1
C					G	2	2			C				1	G800				
C				2	A					C				2	U			1	
C				3	A					C				3	A				
C				4	U					U740				2	G				
G				4	U				1	G					U				
G					C				2	G					C				
G		1[b]			C680				1	A				2	C				2
C					A				1	C				1	A				3
U					G		1			G				1	C				2
C620					G		1			A					G				
A					U					A				1	G810				
A					G	1	2			G				1	C				
C					U					A					G				

[a] The enzymes used in this table hydrolyze phosphodiester bonds of RNA, leaving either 3′-phosphates and 5′-hydroxyls (T_1 and T_2) or 5′-phosphates and 3′-hydroxyls (V_1). In this table, cutting at a particule base refers to hydrolysis of the phosphodiester to the 3′ side of the base. [b] The presence of these cuts is not consistent from gel to gel. [c] At least four cuts of intensity 1–3 are found among these bases; their precise location is uncertain because of band compression. [d] G721 and G722 are unresolved; cutting may occur at one or both sides. [e] At least two bands, intensity 2–3, are found between 719 and 722, most likely toward the 5′ side of the sequence. [f] It is uncertain whether this cut is at 723 or 724; its intensity is 2.

F61 RNA into four main sections: the 588–651 hairpin, 655–751 hairpin, long-range interactions, and 769–810 hairpin. The structures shown in Figures 5–8 are taken from the most recent Noller–Woese proposal (Woese et al., 1983), with our results superimposed. Helical segments are assigned Roman numerals for reference. Two other groups have also proposed structures for the 16S RNA (Steigler et al., 1981; Maly & Brimacombe, 1983); differences between these proposals and

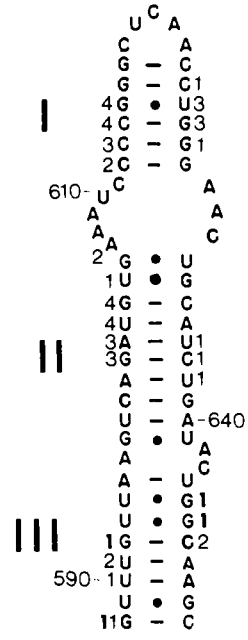

FIGURE 5: Secondary structure of bases 588–651 in the 16S RNA sequence, according to Woese et al. (1983). Enzyme reactivities from Table I are indicated: T_1 RNase, boldface numbers; V_1 nuclease, lightface numbers.

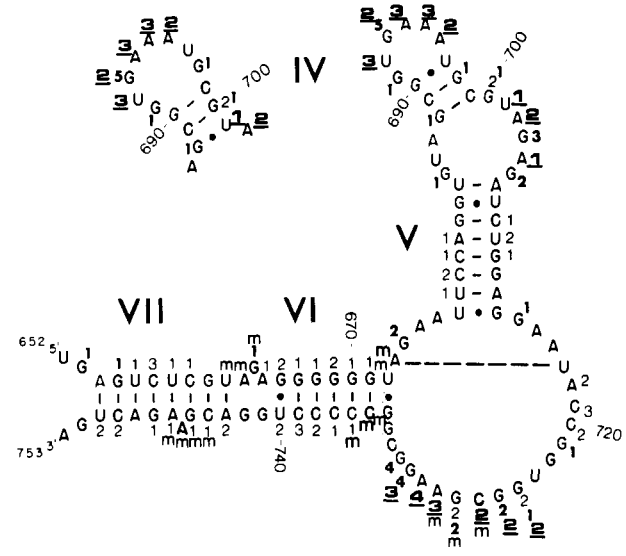

FIGURE 6: Secondary structure of bases 651–753 in the 16S RNA sequence, according to Woese et al. (1983). (Inset) An alternate pairing scheme for bases 687–702. T_1 and V_1 nuclease reactivities from Table I are indicated in the same fashion as Figure 5; T_2 RNase cuts are indicated by boldfaced underlined numbers. Bases strongly reactive toward methidiumpropyl-EDTA–Fe(II) (Kean et al., 1984) are indicated by "m".

the Noller–Woese proposal are minor and will be mentioned when relevant.

Hairpin at Bases 588–651. Bases 588–651 appear to fold into a hairpin of three helices and two bulge loops. Helix III is marginally stable in the absence of Mg^{2+}: T_1 RNase cuts weakly at all the Gs in this helix at 37 °C, and these cuts become much stronger at 60 °C. With added Mg^{2+} the helix is substantially stabilized, as expected (i.e., no change in T_1 digestion level occurs between 37 and 60 °C). However, these Gs are still detectably cut with Mg^{2+} present. This suggests that the base pairs in helix III occasionally open long enough to be trapped by T_1 RNase, even when the helix is far below its melting temperature. Mandal et al. (1979) have shown that a significant fraction of poly(A)-poly(U) base pairs are open well below the helix denaturation temperature; G-U pairs or some aspect of the RNA tertiary structure may induce similar behavior in the helix III.

The fact that Gs in both strands of helix III become more susceptible to T_1 RNase at 60 °C helps to confirm this pairing scheme. Helix III has the potential of stacking with helix VIII of the long-range structure to form one longer, continuous helix; this will be discussed further below.

The phylogenetic data suggest that the ribosome requires only modest stability of helix III. In the 16S-like RNAs from a number of organisms the interior loop between helices II and III is expanded, leaving as few as four base pairs in helix III, or in some cases, helix III contains a mismatch [e.g., *Z. mays* chloroplast (Schwarz & Kössel, 1980); *E. gracis* chloroplast (Graf et al., 1982)].

Once helix III is defined, helices I and II are the only plausible base pairings possible within the remaining loop. Helix I, with five G-C pairs, is extremely stable; the six paired G residues show up only faintly after digestion with T_1 RNase in 8 M urea at 50 °C. V_1 nuclease digestion confirms that this helix also forms under standard conditions. Helix II is also confirmed by V_1 nuclease cuts; those at 601–603 are among the strongest in the molecule. The V_1 nuclease cuts on the opposing strand of helix II, at 635–637, are extremely weak, which may indicate that the nuclease is sterically blocked by the folding of the RNA.

The two consecutive G-U pairs at the end of helix II should not be particularly stable (Tinoco et al., 1973; compare with helix III) but are not digested by T_1 RNase. Different results were obtained by Müller et al. (1979), who isolated the RNA fragments protected from RNase digestion by proteins S8 and S15 and found that the consecutive G-U pairs in helix II are sensitive to RNase A and kethoxal (both single strand specific structure probes). However, their RNA fragment was missing bases 611–631 (helix I and part of the adjacent interior loop), which may have allowed the G-U pairs to "fray". We also find that V_1 nuclease cuts very strongly at 601–603, on the 5′ side of these G-U pairs, and again in the bulge loop at A607. There is no base pairing scheme that includes 607 as part of a Watson-Crick helix and is also consistent with the other nuclease sensitivities. V_1 nuclease is known to cut at some bases that are stacked but not base paired in tRNAs (Auron et al., 1982). Thus, we suspect that base 607 is stacked on the end of helix II in a roughly helical conformation.

Hairpin at Bases 655–751. Nuclease cuts in this region (Figure 6) are largely consistent with the Noller–Woese structure, and there are several interesting features. The affinity cleavage reagent methidiumpropyl-EDTA–Fe(II) intercalates between double-helical base pairs and cuts both strands (Hertzberg & Dervan, 1982). We show in the following paper (Kean et al., 1985) that this reagent binds with high affinity to only a few sites in the F61 RNA. Sets of cuts around bases 660–661 and 746–747 imply the existence of helix VII with intercalation at or near base pairs C660–G745 and G661–C744. The helix is unusual in having a single base bulge. This feature is highly conserved among 16S RNAs, though its exact position along the helix varies (Woese et al., 1983). In the *E. coli* 16S sequence, structures with either A746 bulged and A747 paired or A747 bulged and A746 paired are possible and would appear to be roughly equivalent thermodynamically. However, V_1 nuclease clearly cuts on both the 3′ and 5′ sides of A747 but not on the 3′ side of A746, which suggests that the structure drawn is the preferred one.

Helix VI contains an unusual run of five G-C base pairs. An alternate structure can be written in which the pairs "slip" by one so that A665 pairs with U740 and G670 with C735;

this structure was originally proposed by Noller & Woese (1981) and later revised when more sequences became available (Woese et al., 1983). All six G residues from 666 to 671 are protected from T_1 RNase, which is more in line with the structure drawn than the alternate structure. While V_1 nuclease cuts several times in the G_6 sequence, the intensity varies considerably, which argues that the helix is not uniform in structure.

Helix V is perfectly consistent with both the single-strand nuclease and V_1 nuclease data. The remaining loop of RNA, bases 685–705, could form several alternative short helical structures. There is strong comparative sequence data for the pairing shown in Figure 6 (Woese et al., 1983). An alternate scheme with approximately the same free energy of formation is shown as an inset in Figure 6. Maley & Brimacombe (1983) favor the addition of two A-U pairs at one end of helix V, leaving G700 bulged. In the absence of other interactions, the extra AU-AU and AU-GC base stacks (−3.4 kcal) approximately compensate for the single base bulge (+3 kcal) (Tinoco et al., 1973). The Maley and Brimacombe structure appears to be ruled out by the T_2 RNase cuts at U701 and A702. The only positive evidence we have for secondary structure in the region is a single V_1 nuclease cut at G700, which favors the alternate pairing scheme.

Cutting by T_1 RNase in the region from 685 to 705 varies considerably in intensity (see Figure 4), which may afford some clues to the RNA folding. Evidence for the substrate requirements of T_1 RNase comes from a crystal structure of the enzyme complexed with 2′-GMP (Heinemann & Saenger, 1982) and structure mapping studies with yeast $tRNA^{Phe}$ (Lockard & Kumar, 1981). The former shows that recognition of a G involves stacking of a tyrosine against the G and hydrogen bonding at O^6 and N^1; these interactions imply that the optimum substrate G is rather exposed and unstructured. Digests of $tRNA^{Phe}$ however, show that Gs that are hydrogen bonded at O^6 or N^1 (G15, G18, and G19; note that G19 is fully Watson–Crick hydrogen bonded) and stacked in tertiary structures can be cleaved. This could be either because the enzyme does not require all the interactions to have some activity or because the enzyme is able to trap the G in a transient open, unstructured state. Only Gs in the tRNA cloverleaf helices are completely resistant to T_1 cleavage.

Two sites in the 685–705 sequence are extremely labile to T_1 RNase, G703 and G693. On the basis of the above arguments about T_1 specificity, these bases must have little or no stacking or hydrogen-bonding interactions. This is probably because they are at sharp bends at the ends of hairpins. These sites are also rather sensitive to kethoxal in intact, active 30S ribosomal subunits (Noller, 1974; Woese et al., 1983); given their reactivity in the F61 RNA fragment, presumably their exposure in subunits is purely a consequence of local RNA structure. Six of the remaining seven Gs in this sequence are all reproducibly cut by T_1 RNase, some only very weakly. Given the results obtained by Lockard & Kumar (1981) with $tRNA^{Phe}$, these weaker cuts do not rule out important hydrogen-bonding and stacking interactions for these Gs or even Watson–Crick pairing (as in the case of G19 in $tRNA^{Phe}$). We suspect that neither of the short, three base pair helices shown in Figure 6 would completely suppress T_1 cutting. T_2 RNase seems to have a more stringent requirement for extended, single strands, as it cuts at very few places in the F61 sequence, almost always at or near strong T_1 cuts.

The reactivities of the bases in the loop from 714 to 733 show that this region must have a specific structure. Several bases between 719 and 721 are cut by V_1 nuclease, indicating helical structure (because bands are very close spaced in this part of gels with 3′-end-labeled RNA, the precise location of these cuts is somewhat uncertain). T_1 RNase again shows a pattern of cuts through the entire loop and intense cuts only at G731 and G732. Adjacent to these strong T_1 cuts, T_2 RNase cuts bases from 724 to 730 very strongly but curiously skips G727 entirely. G727 is cut moderately by both T_1 and V_1 nucleases. The methidiumpropyl-EDTA–Fe(II) intercalating cleavage reagent discussed in detail in the following paper (Kean et al., 1985) also cuts strongly around G727. This reagent binds only to helical regions of tRNA (Kean et al., 1985). Altogether these data suggest that bases 724–731 are in an extended, single-stranded conformation *except* for the middle base of the sequence, which is involved in some structure.

It is difficult to account for the V_1 nuclease cuts in this loop without invoking the ability of V_1 to cut at bases with substantial tertiary structure but not part of a regular helix (Auron et al., 1982). A computer search of the base-pairing possibilities of the 714–731 sequence with other parts of the F61 RNA revealed no plausible secondary structures. In addition, recent results with a smaller RNA fragment, bases 648–759, give the same pattern of V_1 and T_1 cuts in this region (J. Vartikar and D. E. Draper, unpublished observations), which limits the pairing possibilities to this shorter sequence. We therefore conclude that tertiary interactions in the 714–731 region constrain the RNA to a helix-like conformation. Since T_1 RNase may cut at bases involved in tertiary structure, as discussed above, the weaker cuts in this region are not inconsistent with this conclusion.

Phylogenetic comparisons also suggest some structure for this bulge loop, but the data are ambiguous (Woese et al., 1983). In some RNAs helix V appears to be extended by several base pairs, so that the bulge at 673–676 is paired with 714–718. The only feature that is actually conserved in all RNAs examined is the complementarity between bases 673 and 717 (indicated by a dotted line in Figure 6). These data suggest that a definite structure is required in this region but that it may draw on different proportions of secondary and tertiary interactions in different RNAs. Rather than looking for compensatory Watson–Crick base changes between sequences in this region, it may be worthwhile to look for compensatory acceptor and donor hydrogen-bonding possibilities. For instance, a pair of hydrogen bonds between N^1 and O^6 of G with O^4 and N^3 of U could be replaced by hydrogen bonding between identical positions on A and C. (A and C substitute for G732 and U722, respectively, in some 16S RNA sequences). However, the large number of hydrogen-bonding possibilities between bases make this kind of argument difficult to pursue convincingly without a very large base of sequence variants.

Long-Range Interactions. Bases toward the 5′ and 3′ ends of the F61 RNA pair to form two helices in all of the secondary structure models proposed (Figure 7A). Our structure mapping results are not entirely consistent with this pairing: T_1 RNase cuts weakly but reproducibly 4 times between G760 and G765, in what should be a rather stable helix, and V_1 cuts several times in the bulge loop between helices VIII and IX. We therefore searched for alternative pairings that might account for the data and found the structure shown in Figure 7B. The two secondary structures (Figure 7A,B) are of roughly equal thermodynamic stability. The alternate structure is supported by much of the structure mapping data, particularly the V_1 cuts from 563 to 570. However, three Gs in the middle of the same sequence (566–568) are also sus-

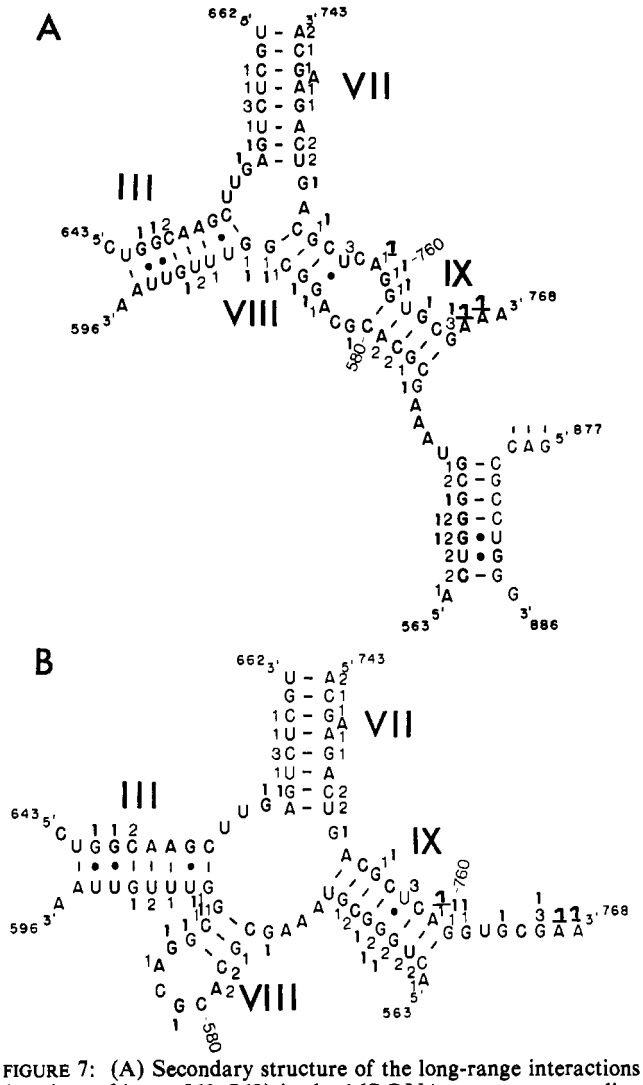

FIGURE 7: (A) Secondary structure of the long-range interactions (portions of bases 563–768) in the 16S RNA sequence, according to Woese et al. (1983). The sequence in light face (bases 877–886) is not present in the F61 RNA fragment. (B) An alternate secondary structure for the same region. Enzyme reactivities from Table I are indicated as in Figure 6.

ceptible to T_1 RNase. These data can be satisfactorily explained if we assume that both base-pairing schemes shown exist in equilibrium; the digestion patterns we observe are then superpositions of the nuclease sensitivities of the two structures. The only inconsistency is a weak V_1 cut at A583, which is not helical in either structure; all the other cuts support one structure or the other. We therefore conclude that both structures are present under our digestion conditions at 37 °C.

There has been speculation that conformational "switches" between two alternate structures are functionally important in ribosomal RNAs (Woese et al., 1983; Thompson & Hearst, 1983). However, the alternate structure of Figure 7B may not be relevant to the intact 16S RNA structure. In the Noller and Woese models of 16S structure bases 564–570 are paired with 880–886 [through Maly & Brimacombe (1983) point out that the evidence for this helix is dubious]. Our F61 RNA fragment ends at 869 and thus does not have the potential to form this helix. It is then possible that in the intact 16S RNA 564–570 would be taken up in pairing with 880–886 and not have the opportunity to form the structure of Figure 7B; i.e., the equilibrium would be shifted in favor of the structure in 7A. Protein binding could also shift the equilibrium in intact ribosomes. Whether or not the alternate interaction (Figure 7B) is functionally significant, it is an intriguing region for

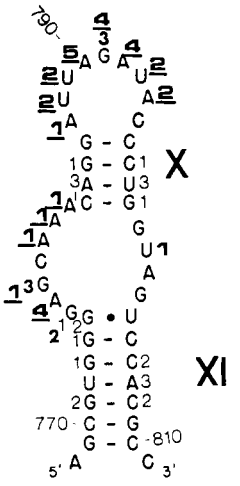

FIGURE 8: Secondary structure of bases 769–810 in the 16S RNA sequence, according to Woese et al. (1983). Enzyme reactivities from Table I are indicated as in Figure 6.

studying the thermodynamic and conformational possibilities of RNA.

Hairpin at Bases 769–810. The T_1, T_2, and V_1 nuclease cuts in this region are exactly as predicted by the Noller–Woese proposal (Figure 8), with the exception of one V_1 cut which extends one base past the end of a helix (G776). This hairpin is probably not essential for S8 or S15 binding but may be required for S6 and S18 assembly into the ribosome (Gregory et al., 1984).

A-G Pairing. Woese et al. (1983) have noted a number of positions in the ribosomal RNAs where juxtapositions between an A and a G are conserved in a helix. The most striking example is the set of helices near the 3′ terminus of 16S RNAs (1408–1490), which contains many internal G-U and A-G juxtapositions in sequences from all organisms. Recent NMR studies of two different short DNA helices have also established that pairing does occur between G and A with both bases in the anti conformation (Kan et al., 1983; Patel et al., 1984). Thus, the possibility of A-G pairing in RNA must be taken seriously. However, we have been unable to detect the formation of G-A pairs in poly(A)-poly(U,G) helices (D. E. Draper and D. Press, unpublished observations) under conditions which allow ready formation of I-A pairs in similar polymers (Lomant & Fresco, 1975). Therefore, G-A pairs must be rather labile.

Woese et al. (1983) have suggested that two A-G pairs form between helices VI and VII, to form one unusually long helix (about 1.5 turns), with G664 bulged. Given the weakness of G-A pairs, this seems a rather unstable structure in the absence of other interactions. In our experiments G741 and G742 are rather well protected from T_1 RNase, while G664 is accessible. We lack any positive evidence for A-G pair formation, however, since V_1 nuclease does not cut at either putative pair, although it does cut at the flanking A-U and G-U pairs. Müller et al. (1979) examined the kethoxal reactivity of Gs in a smaller 16S RNA fragment and found that G741 and G664 are reactive, excluding the possibility of one G-A pair. However, the fragment examined was very small with internal deletions (bases 672–731 were lacking); it is possible that other structures help stabilize G-A pairs at these positions. The conformation of the junction between helices VI and VII must be considered uncertain at present.

Stability of Structures in the F61 RNA. Comparison of T_1 RNase digestion patterns at 37 and 60 °C helped establish the pairing of helix III; the long-range helices also denature in this temperature range. Gralla & Crothers (1973) have

compiled tables of ΔH and ΔS values for different base-pair stacks and loops from which the thermal stability of a helix can be estimated; it is of interest to compare these predictions with the observed stabilities of the helices in the F61 RNA fragment. Much higher stability than predicted for a helix would suggest substantial contributions from tertiary interactions. As a rough approximation, we have calculated the stability of each helix in the F61 structure (presuming the Noller–Woese pairing scheme) using these tables and assuming that all other helices are present when the helix in question denatures. Since the Gralla & Crothers (1973) parameters refer to 1 M NaCl, we have adjusted the calculated T_m's to our standard buffer conditions (0.1 M NaCl) by substracting 20 °C. We emphasize that these calculations are quite approximate; ΔS estimates for loops are particularly uncertain (Tinoco et al., 1973).

Helix IV, with only three base pairs, has a calculated T_m of 67 °C. With this very short helix the calculation is particularly sensitive to the ΔS parameter for loops, and the T_m may be off by ±30 °C; we therefore do not know whether to expect this helix to be denatured in our experiments at 60 °C or not. The only other helix predicted to be unstable is III, with a T_m of 55 °C. If helices III and VIIIA are considered a continuous helix with a bulge loop, the estimated T_m is 62 °C; about the same stability is found for III and VIIIB considered together. The other long-range helices, IXA and IXB, are both predicted to have a T_m of 84 °C. However, if helices III and VIII are denatured, then IX must close a much larger loop, and its stability should drop by about 15 °C, to 69 °C. These very rough calculations of helix stabilities are thus in reasonable agreement with the experimental results: we find that the sequences 566–592, 645–654, and 752–765 all show definite increases in susceptibility to T_1 RNase at the higher temperature, implying that the long-range interactions and helix III are at least partially melting between 37 and 60 °C.

In several other places it appears that helices are starting to fray from the ends at the higher temperature [e.g., the G-U pair at the end of helix X (Figure 4)]. Under more physiological conditions, with 10 mM Mg^{2+} present, no fraying or denaturing of helices is observed between 37 and 60 °C.

Conclusions

Comparison of Structure Mapping and Comparative Sequence Results for 16S RNA Structure. The secondary structure we deduce for the F61 RNA fragment is in excellent agreement with the structures that have been deduced for intact 16S ribosomal RNA by comparison of sequence variants. The two large hairpins that dominate the structure (Figures 5 and 6) are unambiguously present in the fragment. One of the two alternate long-range interactions that exists in the fragment is the same as predicted by sequence comparisons. The only uncertainties in the interpretation of our data are in the two regions that probably contain substantial tertiary interactions (685–705 and 714–733).

Sequence comparisons must refer to the conservation of RNA structure in *intact* ribosomes; bound proteins and substrates may certainly constrain the RNA to a different structure than thermodynamically preferred in the isolated molecule. Our structure mapping results, in contrast, have been obtained with RNA that is both devoid of protein and only a fragment of the full molecule. The two different kinds of studies need not refer to the same structure. The fact that the secondary structure of our fragment is in such good agreement with the sequence comparison results is strong support for the idea of independently folding domains in the 16S RNA and gives us some confidence that further studies of tertiary interactions and protein binding with the F61 fragment will be relevant to the RNA structure in intact molecules and ribosomes.

Limitations of Structure Mapping Experiments. The study reported here establishes the major secondary interactions in the F61 RNA and suggests that some regions have specific tertiary structures. Unfortunately, the structure mapping approach, potentially the most powerful tool available for rapidly delineating the structure of larger RNA molecules, is limited by two difficulties to mapping only major RNA secondary structures unambiguously. One is the difficulty of interpreting the structure of regions susceptible to both single- and double-strand specific reagents. There are at least three possible explanations when this arises: (i) The region is only marginally stable and is starting to denature; (ii) two different secondary structures are present in equilibrium; (iii) The reagents lack absolute specificity for single- or double-stranded structures. We have required all three of these possibilities in interpreting our data. The predicted marginal stability of helix III, and its apparent denaturation at higher temperature make (i) the most likely explanation for both V_1 and T_1 nucleases cutting in this region. The absence of any suitable secondary structures for the 714–733 region forced us to assume the presence of a tertiary structure recognized by both V_1 and T_1 nucleases, though we cannot rule out the possibility that there are two or more tertiary structures in equilibrium. Last, our finding of two different base-pairing schemes which together accounted for the digestion patterns in the long-range interactions made explanation ii seem particularly attractive for that region. In all three of these regions we have made reasonable arguments in favor of the interpretation used, but we are not able to definitively rule out other explanations.

A second major difficulty with structure mapping is the availability of suitable reagents, especially ones with precisely defined reactivities. The majority of residues in an RNA molecule are probably hydrogen bonded and stacked in a specific structure. Yet all the chemical structure probes available (Peattie & Gilbert, 1980) and all but one of the enzymes available prefer single-stranded, unstacked residues. Only V_1 nuclease is specific for double-helical RNA, and its cleavage is occasionally ambiguous because it may recognize bases in highly structured regions of tertiary structure. It is thus sometimes difficult to obtain positive evidence for the existence of a structure. The affinity cleavage intercalator methidiumpropyl-EDTA–Fe(II) (Hertzberg & Dervan, 1982) is also useful in some situations for mapping secondary structures (Kean et al., 1985), but many more reagents with specificity for particular RNA conformations need to be devised before structure mapping increases much in precision.

References

Auron, P. E., Weber, L. D., & Rich, A. (1982) *Biochemistry 21*, 4700–4706.

Boyer, H. W., & Roulland-Dussoix, D. (1969) *J. Mol. Biol. 41*, 459–472.

Brosius, J., Dull, T. J., Sleeter, D. D., & Noller, H. F. (1981) *J. Mol. Biol. 148*, 107–127.

D'Alessio, J. M. (1982) in *Gel Electrophoresis of Nucleic Acids* (Rickwood, D., & Hames, B. D., Eds.) pp 173–197, IRL Press, Oxford.

Dennis, P. P., & Nordan, D. H. (1976) *J. Bacteriol. 128*, 28–34.

Donis-Keller, H., Maxam, A., & Gilbert, W. (1977) *Nucleic Acids Res. 4*, 2527.

Garrett, R. A., & Oleson, S. O. (1982) *Biochemistry 21*, 4823–4830.

Graf, L., Roux, E., & Stutz, E. (1982) *Nucleic Acids Res. 10*, 6369–6381.

Gralla, J., & Crothers, D. M. (1973) *J. Mol. Biol. 73*, 497–511.

Gregory, R. J., Zeller, M. L., Thurlow, D. L., Gourse, R. L., Stark, M. J. R., Dahlberg, A. E., & Zimmermann, R. A. (1984) *J. Mol. Biol. 178*, 287–302.

Heinemann, U., & Saenger, W. (1982) *Nature (London) 299*, 27–31.

Herrmann, R., Neugebauer, K., Pirkl, E., Zentgraf, H., & Schaller, H. (1980) *Mol. Gen. Genet. 177*, 231–242.

Hertzberg, R. P., & Dervan, P. B. (1982) *J. Am. Chem. Soc. 104*, 313–315.

Hogan, J. J., & Noller, H. F. (1978) *Biochemistry 17*, 587–593.

Kan, L.-S., Chandrasegaran, S., Pulford, S. M., & Miller, P. S. (1983) *Proc. Natl. Acad. Sci. U.S.A. 80*, 4263–4265.

Kean, J. M., White, S. A., & Draper, D. E. (1985) *Biochemistry* (following paper in this issue).

Laskey, R. A. (1982) *Methods Enzymol. 65*, 363–371.

Lockard, R. E., & Kumar, A. (1981) *Nucleic Acids Res. 19*, 5125–5140.

Lockard, R. E., Alzner-Deweerd, B., Heckman, J. E., MacGee, J., Tabor, W., & RajBhandary, U. L. (1978) *Nucleic Acids Res. 5*, 37.

Lomant, A. J., & Fresco, J. R. (1975) *Prog. Nucleic Acid Res. Mol. Biol. 15*, 185–218.

Maly, P., & Brimacombe, R. (1983) *Nucleic Acids Res. 11*, 7263–7286.

Mandal, P., Kallenbach, N. R., & Englander, S. W. (1979) *J. Mol. Biol. 135*, 391–411.

Maniatis, T., Fritsch, E. F., & Sambrook, J. (1982) *Molecular Cloning*, Cold Spring Harbor Laboratory, Cold Spring Harbor, NY.

Maxam, A. M., & Gilbert, W. (1980) *Methods Enzymol. 65*, 499–560.

Müller, R., Garrett, R. A., & Noller, H. F. (1979) *J. Biol. Chem. 254*, 3873–3878.

Noller, H. F. (1974) *Biochemistry 13*, 4694–4703.

Noller, H. F. (1980) in *Ribosomes: Structure, Function, and Genetics* (Chambliss, G., et al. Eds.) pp 3–19, University Park Press, Baltimore.

Noller, H. F., & Woese, C. R. (1981) *Science (Washington, D.C.) 212*, 403–411.

Patel, D. J., Kozlowski, S. A., Ikuta, S., & Itakura, K. (1984) *Biochemistry 23*, 3207–3218.

Peattie, D. A., & Gilbert, W. (1980) *Proc. Natl. Acad. Sci. U.S.A. 77*, 4679–4682.

Schwarz, Z., & Kössel, H. (1980) *Nature (London) 283*, 739–742.

Shen, W.-F., Squires, C., & Squires, C. L. (1982) *Nucleic Acids Res. 10*, 3303–3313.

Steigler, P., Carbon, P., Zuker, M., Ebel, J. P., & Ehresmann, C. (1981) *Nucleic Acids Res. 9*, 2153–2172.

Thompson, J. F., & Hearst, J. E. (1983) *Cell (Cambridge, Mass.) 33*, 19–24.

Tinoco, I., Borer, P. N., Dengler, B., Levine, M. D., Uhlenbeck, O. C., Crothers, D. M., & Gralla, J. (1973) *Nature (London) 246*, 40–41.

Tritton, T. R., & Crothers, D. M. (1976) *Biochemistry 15*, 4377–4385.

Ungewickell, E., Garrett, R., Ehresmann, C., Steigler, P., & Fellner, P. (1975) *Eur. J. Biochem. 51*, 165–180.

Woese, C. R., Gutell, R., Gupta, R., & Noller, H. (1983) *Microbiol. Rev. 47*, 621–669.

Yamamoto, K. R., Alberts, B. M., Benziger, R., Lawhorne, L., & Treiber, G. (1970) *Virology 40*, 734–744.

Zimmermann, R. A. (1974) in *Ribosomes* (Nomura, M., Tissieres, A., & Lengyel, P., Eds.) pp 225–269, Cold Spring Harbor Laboratory, Cold Spring Harbor, NY.

Zimmermann, R. A., Muto, A., Fellner, P., Ehresman, C., & Branlant, C. (1972) *Proc. Natl. Acad. Sci. U.S.A. 69*, 1282–1286.